GFRP-sheet strengthened RC beams after seawater immersion under monotonic and fatigue loads

Arbain Tata[1,*], *Anthonius* Frederik Raffel[1], *Muhammad* Ihsan[2], and *Rudy* Djamaluddin[3]

[1]Department of Civil Engineering, Universitas Khairun, Ternate, Indonesia
[2]Sekolah Tinggi Teknik Baramuli, Pinrang, Indonesia
[3]Department of Civil Engineering, Universitas Hasanuddin, Makassar, Indonesia

Abstract. This study aims to analyse glass fibre reinforced polymer (GFRP) reinforcement on reinforced concrete beams under fatigue and monotonic loads influenced by sea water. The research was conducted in the laboratory on flexural concrete beams with the quality of $f'c$ = 25 MPa. One normal concrete flexural beam (BN) with repetitive load was without seawater and no reinforcement. One flexural beam was without sea water immersion but with GFRP-reinforcement. Another flexural beam reinforced by GFRP sheets is immersed in a pond containing seawater with time variations up to 12 months. The test was performed with a fatigue load of 1.25 Hz frequency to failure. The results showed an increase in capacity due to 58.3% for GFRP-reinforcement. There is a decrease in the capacity of GFRP sheet influenced by seawater immersion. The same trend with the decrease in ductility occurred in the flexural beam to 14% due to seawater immersion. Maximum beam failure repetition occurred at 1,230,000 cycles on beam with reinforcement (BF). The failure occurring in the flexural beam was preceded by the failure of the attachment between the concrete and the GFRP sheet at the load centre (mid of span) slowly to the support until failure (debonding) initialized. The GFRP-S bonding capacity to the concrete skin has decreased in 12 months by 15%. Therefore, there is a significant effect of decreasing strength due to fatigue loads and seawater immersion.

1 Introduction

Fiber reinforced polymer (FRP) materials have been applied widely in the enhancement of structural integrity. Carbon fiber reinforced polymers (CFRP) applied in bridge retrofitting have been proven capable and effective in improving durability and capacity to withstand a static load of concrete beam [1, 2]. As construction material technology advances, the applications of Carbon Fiber Reinforced Plastics (CFRP) have been well functioned in rehabilitation and retrofitting of the concrete structure, particularly of the bridge girders, to improve service capacity of the bridge structure. A study of static and fatigue behavior was conducted on three pairs of the small-scale reinforced concrete girder to investigate effects

* Corresponding author: arbatata@yahoo.co.id

of overloading to increasing fatigue of internally bond carbon fiber (CFRP) lamination, and to understand the mechanism underlying the accumulation of fatigue deterioration of bridge girder strengthened by CFRP under overloading condition [3].

GFRP material is a type of materials with several advantages such as high tensile stress, lightweight and corrosion resistant. Hence it would not contribute additional weight to the structure [2, 4]. The application of this material is quite simpler compared to that of conventional concrete and is considered too environmentally friendly. There is vast research which has been conducted and applied widely in the improvement of the capacity of the flexural beam as a respond to the increase of load requirements, usage alteration, degradation of the structure, and complexity in design as well as construction defects [5-8]. The efficiency of reinforcement with CFRP on corroded girders as indicated by an increase in fatigue life of reinforced beams when compared to unreinforced beams [9].

There are plenty of tests on beam with GFRP reinforcement on the tensile side by using static loading. However, in reality, girders on bridge bear repetitive loads from passing vehicles where this type of loading is the most dominant factors in the ruptures of bridges. Some research proved that repetitive loading could induce ruptures or failures of structure even in a lower magnitude of loading far below ultimate flexural capacity [10]. Other have used Glass Fiber Reinforced Plastics (GFRP) to increase the flexural strength of beam [6]. In this regard, the innovation of durability of reinforced concrete beam strengthened by GFRP due to fatigue load is still needed to be investigated further. Therefore, in this research, GFRP Sheets were applied as reinforcement for flexural beam under fatigue and static load as well as immersion of sea water.

2 Literature review

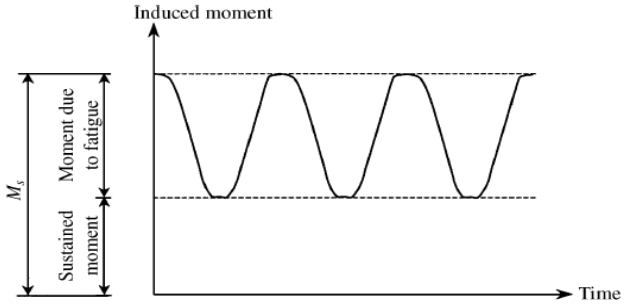

Fig. 1. Moment capacity of stress limit of GFRP.

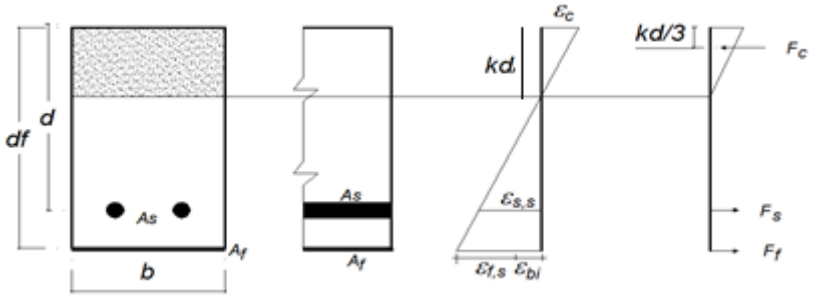

Fig. 2. Elastic strain and stress distribution (a) cross section, (b) strain, (c) stress.

The design procedure for FRP reinforced beam in this research follows ACI 440.2R-08 Guide for the Design and Construction of Externally Bonded FRP System for Strengthening Concrete Structures". The stress-strain condition of concrete beam section is depicted in Fig. 1 illustrates the internal strain and stress distribution for a rectangular section under flexure at the ultimate limit state. The procedure used to calculate the ultimate strength should satisfy strain accountability and force equilibrium and should consider the governing mode of failure. Some calculation procedures can be derived to satisfy this condition.

$$f_{s,s} = \frac{\left[M_s + \varepsilon_{bi} A_f E_f \left(d_f - \frac{kd}{3}\right)\right](d-kd)E_s}{A_s E_s \left(d - \frac{kd}{3}\right)(d-kd) + A_f E_f \left(d_f - \frac{kd}{3}\right)(d-kd)} \quad (1)$$

$$f_{f,s} = f_{s,s}\left(\frac{E_f}{E_s}\right)\frac{(d_f - kd)}{(d-kd)} - \varepsilon_{bi} E_f \quad (2)$$

where $f_{s,s}$ = stress of reinforcing steel, $f_{f,s}$ = bonding capacity of GFRP-S, E_f = elasticity of GFRP-S, and E_s = Modulus Elasticity of reinforcing steel.

3 Methods

3.1 Manufacturing of test specimen

Type of concrete studied was normal concrete with a design the compressive strength of 25 MPa. The compressive and flexural strength of concrete were examined through cylindrical compressive strength test and flexural beam test. The concrete casting was conducted in compliance with the standard. Concrete formwork dismantling was conducted on day three followed by curing which was conducted by covering the specimens with a wet sack for 28 days. All reinforced concrete beam specimens were designed by design standard [8]. Fig. 3 shows the details of the prepared test beam. The concrete beam was prepared in the cross-sectional dimension of 100x150mm with 3,300 mm length.

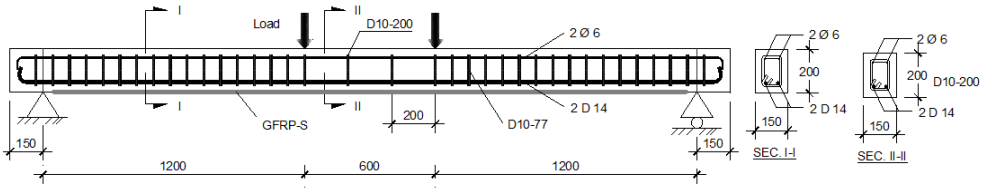

Fig. 3. Details of tested beam.

The beam is designed with 2D14 steel bar as a tensile reinforcement with average yield stress of 421.7 MPa, while D10 stirrup steel bar has yield stress of 410.2 MPa. Steel tensile test data of month 1 and month 2 show no significant difference. The results have complied design yield stress level of 400 MPa. To prevent from sliding failure, reinforcement bar with a diameter of 6 mm is used as stirrups. FRP materials used are glass fiber reinforced polymer-sheet (GFRP-S). The combination of glass fiber and epoxy resin would develop GFRP-S reinforcement on concrete beams. Technical parameters of GFRP-S and properties of epoxy resin used in this research are shown in Table 1 and 2. Application of GFRP-S as beam's reinforcement was conducted at 28 days.

Table 1. Specification of GFRP-S type SHE-51A.

Material properties	Test results
Tensile stress (GPa)	3.24
Tensile modulus (GPa)	72.40
Maximum strain (%)	4.5
Density (gr/cm^3)	2.55
The thickness of fiber (mm)	0.36

Table 2. Properties epoxy resin.

Material properties	Test results
Tensile stress (MPa)	72.40
Young modulus (GPa)	3.18
Bonding stress (MPa)	2.12

The application process for strengthening the beam is on procedures by the standard as shown in Fig. 4. Initially, the surface of the beam at the tensile side was cleaned by polishing its surface. The glass fiber sheet was then cut out according to the desired size and coated with an epoxy resin. Then, the glass fiber sheet was affixed into the surface of concrete after the surface had been coated with an epoxy resin as well. After properly positioned, the sheet material was then sealed off and coated with epoxy resin using a roller that the entire sheet became saturated with an epoxy material. Further, the test material was left dry to make the epoxy resin material harden and fused with glass fiber material to form the GFRP-S attached to the tensile side (bottom side) of the reinforced concrete beam. The simulation pool made has a dimension of 8.30 m in length and 4.30 m in width and 1.15 m in height. The dimensions of the pond are adjusted to the size of the flexible beam to be studied. The detailed picture of the simulation pool can be seen in Fig. 5.

Fig. 4. Applied GFRP sheet.

Fig. 5. Seawater immersion pool.

3.2 Data recording

Fatigue load was tested with fatigue testing instrument with a loading capacity of 100 ton. As shown in Fig. 4, before the testing, strain gauges were affixed into the surface of concrete and surface of GFPR-S to measure the strain in the test specimen during the loading process. Specimen beam was placed on top of two simple supports which behave as

hinge-roll. The load is given into two points at 50 cm distance at the middle of beam's span. The magnitude of the load amount is given through measured by using Load-Cell while the deflection is measured by using LDVT which is placed at the midpoint of beam's span. All measurement instruments are connected into a data tabulation system and connected to the computer to monitor all measured parameters during the loading process. The beam is designed to be loaded by fatigue load with minimum load 4kN (or around 5% from the ultimate flexural capacity) and maximum load 24 kN (or around 45% from the ultimate compressive strain of concrete). The minimum-maximum load pattern was given repeatedly with frequency 1.25 Hz and was given continuously until specimen failure. The data reading was conducted after the beam experiencing repetitive load with a period of 10 cycles, 100 cycles and multiples of 50,000 cycles until beam failure.

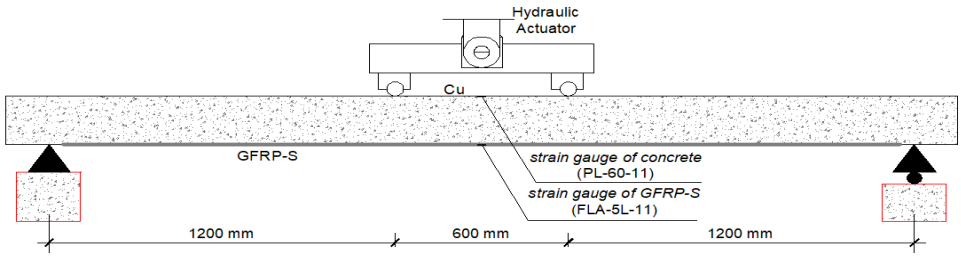

Fig. 6. Details of static and fatigue loading.

Next fatigue tests were conducted when the test beam has been immersed in seawater for 1, 3, 6 and 12 months. Deflection is also measured by using LDVT on the lower part of the beam. Crack patterns were also investigated by using phi gauge. Loading was conducted by the two-point loads on BN and BF. Fatigue load could cause fatigue and failure, with a constant frequency of 1.25 Hz and sine wave model load as depicted in Fig. 6. Sinusoidal fatigue loads were applied in 1 cycle, 10 cycles, 100 cycles, 1000 cycles, 10,000 cycles and subsequent multiplies of 50,000 cycles until beam failure or until reaching 1,000,000 cycles. Loading was given in minimum and maximum for a respective beam of unreinforced type (BN), and GFRP-S reinforced one (BF) with magnitudes of 4-19 kN and 4-24 kN. Minimum load is estimated from a dead load of the beam while maximum loads of 19 kN or 24 kN are estimated from 45% f'c of control beam of the respective type of beam, GFRP-S reinforced and unreinforced. Data are acquired from data logger in every 1 kN load increasing in normal condition. As data recorded, tested beams are continuously observed for development of crack, as well as their failure behavior.

4 Results and discussion

4.1 Behaviour of beams under static load

Before discussion of the behavior of the beam due to fatigue load, the behavior of control beam due to monotonic load will be discussed. This is to evaluate the influence of fatigue loads when compared with the influence of monotonic load. The stiffness of the structure is important. Stiffness restriction is used to keep the structure from over deflection. Stiffness is defined as the force required to produce a unit of displacement and its value is the gradient of the relationship between load and deflection. The stiffness of a concrete beam is a function of the elastic modulus (E) and the moment of inertia (I). In this research, four beams were loaded with monotonic load until the beam is cracked and destroyed immediately as the load increases. The four tested beams are BNK1, BNK2, BFK1, and BFK2 are in Fig. 7.

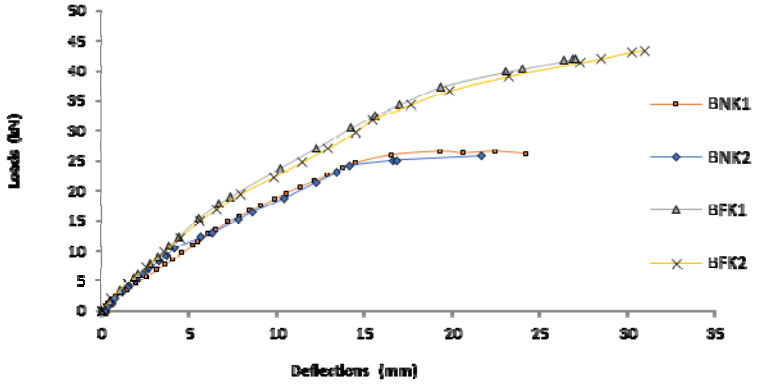

Fig. 7. Relationship of load to deflections of concrete beam BNK1, BNK2, BFK1 and BFK2.

Fig. 7 depicts beam deflection behavior for BNK1, BNK2, BFK1, and BFK2. From the graph, it can be explained that the behavior of each specimen depends on the characteristics of each beam. For BNK1 beam, the loaded relationship at the beginning of loading is still a linear line showing full elastic behavior up to 5.07 kN loading with a deflection of 2.07 mm. As the load increases, the reinforcing steel bar yields with a noticeably larger deflection without an increase in load (load value of 22.90 kN) and a deflection of 14.57 mm. The nonlinear load relation curve to deflection becomes much flatter than before. This occurred until the beam reaches a maximum load of 26.44 kN and deflection of 36.07 mm. As for BNK2 test specimen, the trend is still linear at the beginning of loading showing full elastic behavior before reaching 5.07 kN load with a 1.62 mm deflection. As the load increased, the reinforcing steel bar started to yield which is marked by a large increase of deflection without a significant load increase where the load value is 24.10 kN with a deflection of 14.21 mm, and the nonlinear relationship curve is much flatter than before. This occurs until the beam reaches a maximum load of 24.10 kN and a deflection of 21.67 mm.

Table 3. Comparison of the ductility of BNK and BFK.

Description	Experiment						Displacement Ductility	Average Displacement Ductility
	P_{crack} (kN)	Δ (mm)	P_{yield} (kN)	Δ_{yield} (mm)	$P_{Ultimit}$ (kN)	$\Delta_{ultimate}$ (mm)		
BNK1	5.13	2.66	25.57	15.49	26.09	38.92	2.51	2.42
BNK2	5.07	2.66	22.90	15.87	26.44	37.24	2.34	
BFK1	8.00	3.44	31.24	15.79	42.33	43.25	2.73	2.76
BFK2	8.02	4.74	33.65	15.92	43.73	44.56	2.79	

For BFK1 test object, the trend is still linear at the beginning of loading showing full elastic behavior before reaching 8.00 kN load with a deflection of 3.88 mm. Increasing the load caused steel reinforcement to yield. The large increase of deflection without followed by significant load increase where the load value is 31.24 kN, with a deflection of 15.64 mm, the nonlinear relationship curve becomes much flatter than the previous stage. This occurs until the beam reaches a maximum load of 42.33 kN and the deflection is 26.40 mm. On

BFK2 test object, full elastic behavior occurred before reaching 8.02 kN load with a deflection of 3.61 mm. As the load escalated, the reinforcing steel underwent a yield which is marked by a large increase of deflection without an increase in load which means the load value is 33.65 kN with a deflection of 15.52 mm, where the relationship curve is much flatter than before. This occurs until the beam reaches a maximum load of 43.73 kN and a deflection of 27.29 mm. From table 3 above, it is shown that there are significant differences in the capacity of GFRP-S reinforced beam (BN) when compared to beam without GFRP-S reinforcement (BF) with 58.3% differences.

Ductility is the capacity of structures to withstand enormous deflection without undergoing considerable recession of strength so that the structure in its integrity despite being damaged or initiating to collapse. Ductility factor of building structure μ is the ratio of maximum deviation of the structure of building due to design earthquake effect near collapse condition u to the deviation of the structure at the moment of initial yield y. Mathematically, ductility is defined as the comparison of the displacement parameter of a structure at the time of collapse and displacement when the outer tensile reinforcement undergoes fatigue condition. The displacement ductility is the ratio of deflection of the structure on the initial yield phase (yield) to maximum structural displacement (max = 14.57 mm) [11]. Initial structural yield deflection is obtained on the initial crack of the beam when loaded. Maximum structural yield deflection is obtained when the structure has collapsed. From Table 3, it is obvious that there is a significant increase in the displacement ductility of the reinforced concrete beam (BF) at 14% higher than that unreinforced concrete beam (BN).

$$\varphi_{\Delta} = \frac{\Delta_u}{\Delta_y} \tag{3}$$

4.2 The behaviour of beams under fatigue load with seawater influence

Normal beam (BN) failed at 835,000 cycles. On minimum load level (P = 4 kN), the deflection was still unnoticeable after fatigue loading. However, at the higher load level, the change of deflection is quite significant. On maximum load (19 kN), fatigue load influence increases to 11.03% after the beam experiencing 800,000 cycles of fatigue load.

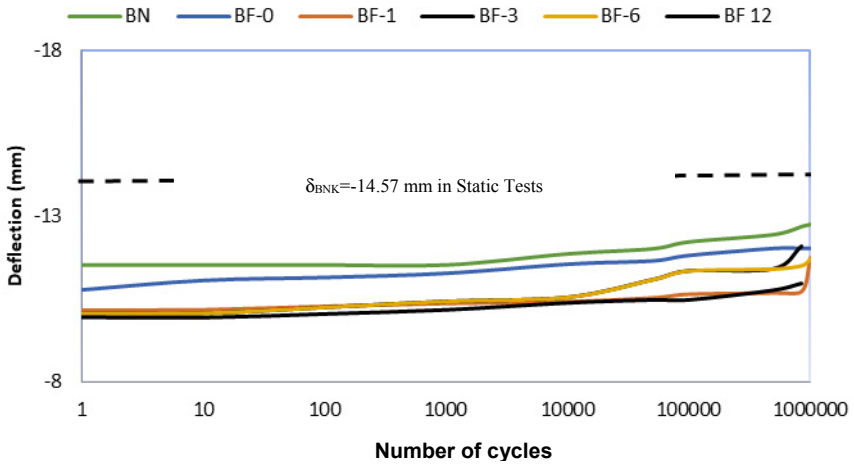

Fig. 8. Relationship of number of cycle and deflection on BN, BF0, BF1, BF3, BF6 and BF12 under maximum load in the mid of span.

What occurred to normal beam without reinforcement also occurred in reinforced concrete beams strengthened with GFRP-S. Fig. 8 shows deflections on GFRP-S strengthened beams for various loading levels after undergoing fatigue loads up to 1,230,000 cycles. The average numbers of cycles, when GFRP-S strengthened beams experienced failure, were 1,000,000 cycles. At the relatively small load level (P = 4 kN) the deflection appears not to be influenced by the fatigue load. At higher load levels the effect of repeated loading has begun to appear. At 14 kN load, there is an increase in deflection after the beam underwent 1,000,000 cycles of fatigue loading. At 24 kN load, the influence of fatigue load is increasingly visible where deflection increased after in loaded 1,000,000 cycles. The effect of fatigue loading after 1,200,000 cycles for different levels of loading tends to decrease as immersion proceeded. This can be indicated by the weakening of the GFRP-S bond to the concrete on the tensile side. In general, structural weakness is also caused by the fatigue load caused by the emergence of microcracks due to repetitive loads.

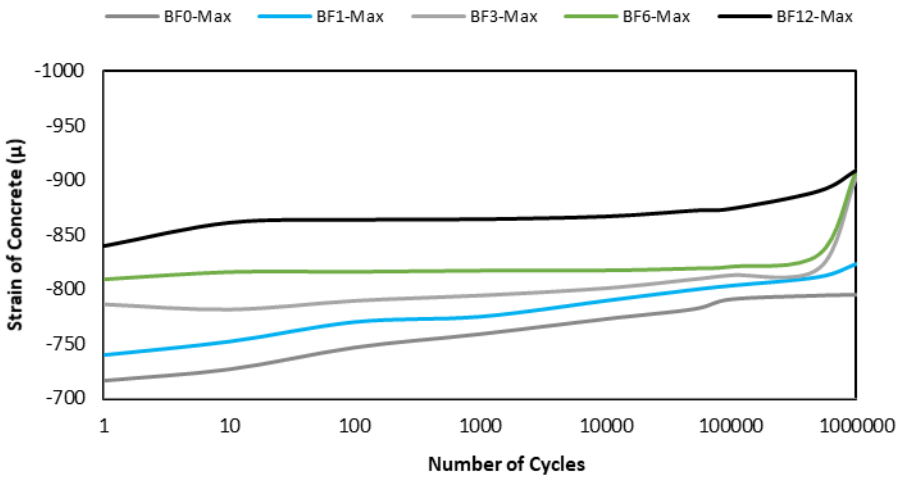

Fig. 9. Relation of concrete strain with a number of cycles for BF0, BF1, BF3, BF6 dan BF12.

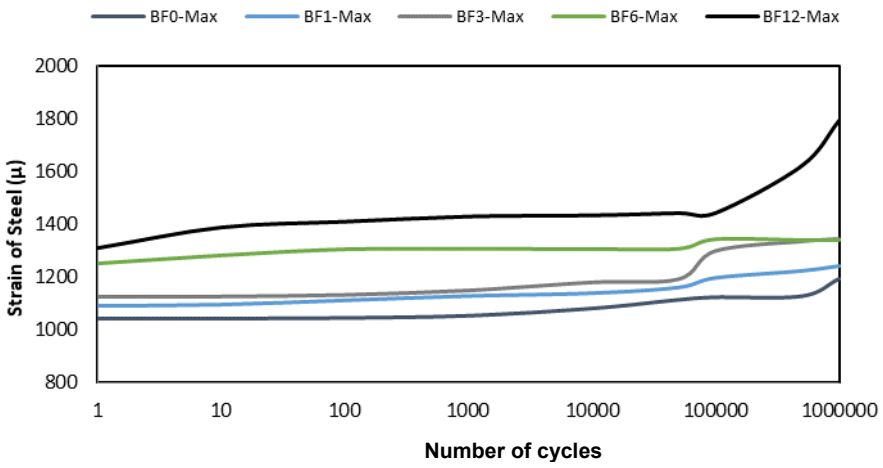

Fig. 10. Relation of reinforcing steel strain with a number of cycles for BF0, BF1, BF3, BF6 and BF12.

Fig. 9 shows compressive strain occurring on the compressed side of the GFRP-S reinforced beam for various loading levels after fatigue load cycles up to 1,000,000 cycles. At BF-0 (before immersed), there is an increase in the compressive strain as some cycles increases from the first cycle to one million cycles at a maximum load of 24 kN with a concrete compressive strain of 716 μ to 795 μ. This shows an increase of compressive strain by 11% due to a fatigue load of a million cycles. As for BF-12 (12-month immersion), there was an increase in compressive strain as some cycles increases from the first cycle to one million cycles at a maximum load of 24 kN with a concrete compressive strain of 1308 μ to 1794 μ. This shows an increase of 37% compressive strain due to a fatigue load of one million cycles. These results indicate that there is an effect of increasing the compressive strain of 26% due to seawater immersion and indicated by the weakening of concrete bonds to GFRP due to seawater immersion or slow crack propagation processes due to repetitive loads.

As shown in Fig. 10, at higher load levels, it appears that the effect of repetitive loading appears were more significant. In contrast to reinforcing steel, at BF-12 the 24 kN (maximum load), the effect of fatigue load appears to be increasingly visible where strain increases after fatigue loads of one million cycles. In the GFRP-S reinforced beam for varying degrees of immersion after undergoing fatigue loading up to one million cycles, at each load level, it shows an increasing strain of reinforcing steel. This indicated a decline in the capacity of bending moments due to the weakening of GFRP-S bonds to the concrete surface due to seawater immersion. At BF0, maximum load was 1044 μ, while on BF12, the strain was 1308 μ in the first cycle. There was a 25% increase in strain due to seawater immersion. Due to the fatigue load on the BF12, a strain on the first cycle was 1308 μ and was 1794 μ when loaded for one million cycles (1,000,000 cycles), while strain increases to 37%.

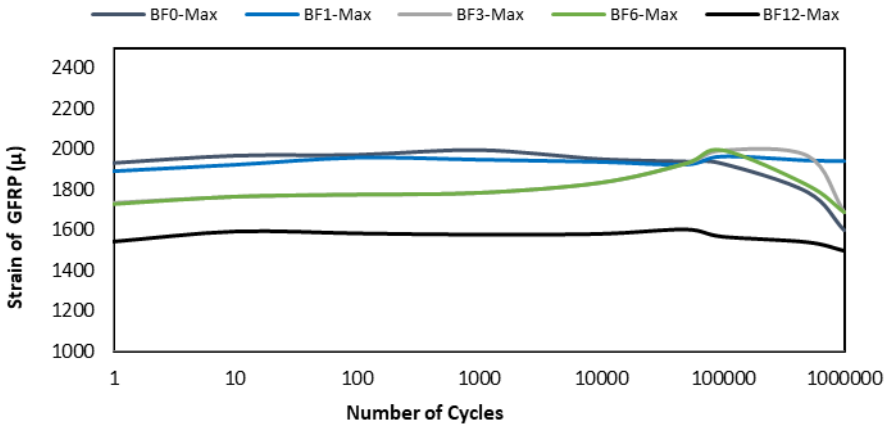

Fig. 11. Relationship of GFRP-S strain with a number of cycles for BF0, BF1, BF3, BF6 and BF12.

The effect of the fatigue load on the GFRP-S strain is shown in Fig. 11. The results show that at the relatively small load level (P = 4 kN) the strain does not change after the fatigue load. However, at higher load levels it appears that the effects of recurrent loading have begun to appear. At 24 kN loading, the influence of fatigue load tends to be more visible where the GFRP-S strain decreases after fatigue loads of one million cycles. This is an indication of weakening composite action of concrete, steel, and GFRP-S. It appears that the weakening of GFRP-S action indicates a weakening of the GFRP-S bonding to the concrete surface.

Table 4. Maximum strain width due to fatigue loads in 500,000 cycles**.**

Beams	Number of cycles to Failure (Cycles)	Strain in 500,000 cycles (μ)			Bonding Capasity of GFRP-S (N/mm^2)
		ε_c (μ) Concrete	ε_f (μ) GFRP	ε_s (μ) Steel	
BF0	1,230,000	794.2	1944.6	1342.1	0.131
BF1	1,000,000	811.4	1820.1	1224.8	0.144
BF3	1,000,000	819.5	1966.3	1334.2	0.132
BF6	1,000,000	832.5	1789.8	1659.0	0.106
BF12	900,000	890.2	1543.2	1606.0	0.111

4.3 Mechanism of concrete beam rupture

The test beams were designed to fail with an under-reinforcement failure pattern. Failure will start with a steel yield which then ended with a concrete rupture on the compressive side. Based on the static test on the beam, the maximum load for the normal beam is 24 kN, and the maximum load for the beam with GFRP-S reinforcement is 42 kN. In fatigue testing, the maximum load given is 19 kN for a normal beam, and the maximum load for the beam with GFRP-S is 42 kN. Although the maximum fatigue load given is only about 45% of the ultimate load, the beam underwent failure after repeated loads of 800 thousand to 1 million cycles. Fig. 12 shows a decreasing strength due to seawater immersion.

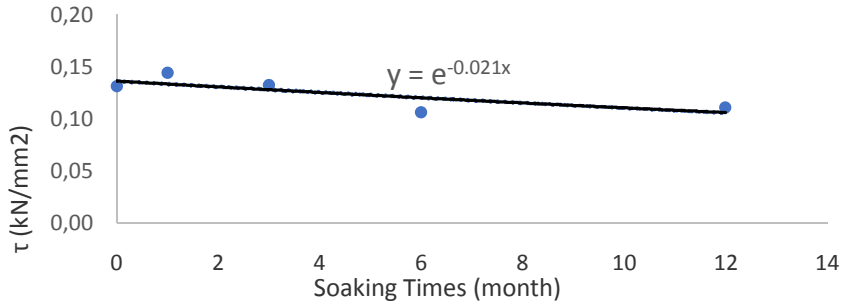

Fig. 12. Relationship of soaking times with bonding capacity.

Fig. 13 shows the condition of the beam undergoing fatigue after repetitive loading. On normal beam, failure occurred in the form of concrete breakdown on the compressive side, while on the beam with GFRP-S failure was preceded by the release of GFRP-S on the tensile side of the beam and followed by the rupture of concrete on the compressive side. The GFRP-S bonding capacity to the concrete skin has decreased in 12 months by 15.5%.

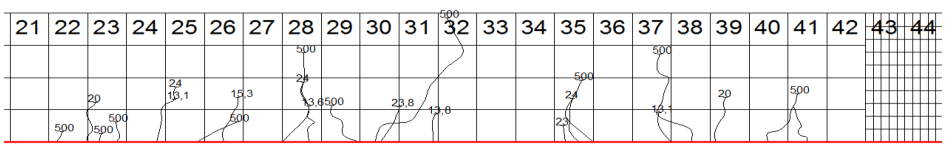

Fig.13. Typical failure due to fatigue loads on BF 500,000 cycles (BF12).

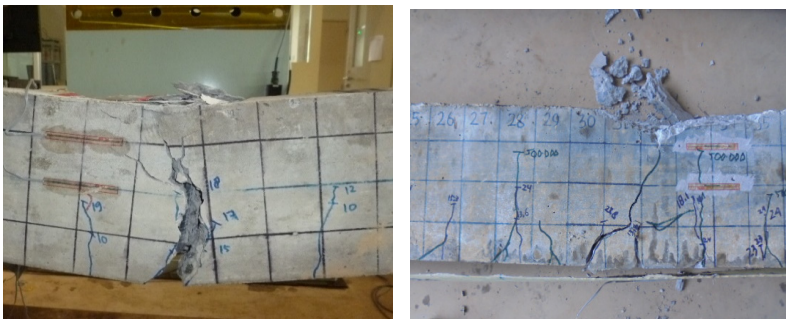

(a) (b)

Fig 14. Typical failure due to fatigue loading on BN and BF (a) The compressive failure of normal beam BN (b) Debonding and compressive failure on GFRP-S Beam GFRP-S.

5 Conclusions

There is a tendency of increasing deflection due to seawater immersion and fatigue load on the one month immersed beam (BF1), three months immersed beam (BF3), six months immersed beam (BF6) and one year immersed beam (BF12) towards unimmersed beam (BF0). This is indicated by the weakening of GFRP-S reinforcement capacity due to seawater immersion and fatigue load. There is a 58.3% increase in moment capacity and a 14% increase in ductility from GFRP sheets reinforcement on flexural beams. There is a significant influence on the increase of strain on the concrete compressive capacity as well as the increase of strain on reinforcing steel due to fatigue loading and seawater immersion. The weakness of the structure due to fatigue and sea water immersion is indicated by the weakening of the bonding between the concrete surface and the GFRP sheet where the composite action of the GFRP sheet is weakened as the number of cycles increases, indicated by the debonding mechanism occurring in the GFRP during ruptures. The GFRP-S bonding capacity to the concrete skin has decreased in 12 months by 15%.

References

1. M. Elkenel, J.J. Myers, J. of Composites for Con. **13**, 2 (2009)
2. M. Sobhy, K. Soudki, T. Topper, J. of Composites for Con. **5**, 4 (2002)
3. X.Y. Sun, J.G. Dai, H.L. Wang, X. Chong, Adv. Steel Con. **11**, 3 (2015)
4. ACI, *Guide for the Design and Construction of Externally Bonded FRP System for Strengthening Concrete Structures* ACI 440.2R-08 (American Concrete Institute, Farmington Hills, 2008)
5. K. Parikh, C.D. Modhera, Int. J. of Civil and Struct. Eng. **2**, 4 (2012)
6. O. Gunes, E. Karaca, B. Gunes. *Proc. of the 8th U.S. National Conference on Earthquake Engineering* (2006)
7. C.G. Papakonstantinou, M.F. Petrou, K.A. Harries, J. of Comp. for Con. **5**, 4 (2001)
8. V.A. Volny, C.P. Pantelides, J. of Composites for Con. **3**, 4 (1999)
9. L. Song, Y. Zhiwu, Indian J. of Eng. & Mat. Sci. **22** (2015)
10. A.B. Richard, C.M. Geoffrey J. of Composites for Con. **3**, 2 (1999)
11. T. Paulay, M.J.N. Priestley, *Seismic design of reinforced concrete and masonry buildings* (John Wiley & Sons, New Jersey, 1992)